

WAVE PROCESSES AND OVERWASH HAZARD ON A HIGH-ENERGY ROCK PLATFORM

Michael A. Kinsela¹, Hannah E. Power², Caio E. Stringari², Murray Kendall², Bradley D. Morris¹ and David J. Hanslow¹

Abstract

The Figure Eight rock platform is a high visitation and hazardous natural attraction located about 1 hour south of Sydney, Australia. The site features unique rock pools that have been weathered into the sandstone platform over thousands of years, which attract local and international visitors who swim in the pools and have their photo taken. A rapid rise in visitation and visitor injuries has prompted an investigation of wave processes and overwash hazard at the site. The method includes morphology and process measurements, and camera monitoring to develop a time series dataset of platform overwashing to analyse in the context of tide and wave conditions. The overall objective of the study is to refine and verify a predictive model for overwash hazard at the site to improve the management of visitor safety.

Key words: coastal hazards and safety, rocky shores, wave modelling, camera monitoring, southeastern Australia

1. Introduction

Rocky shore platforms (hereafter rock platforms) form where erosional processes including wave action cut and plane coastal bedrock exposures. Over time, the erosional processes typically result in a flat to sloping rock platform surface in the vicinity of the shoreline. The morphology of rock platforms is influenced by the composition of the substrate and the prevailing hydraulic conditions, such as the tidal range and wave climate (Sunamura, 1992). Kennedy (2015) reviewed the morphology of rock platforms to develop definitions for key morphological features, in particular the seaward edge. While a continuum of morphologies exists, Sunamura (1992) described the two end members as: platforms that slope uniformly into the sea (type-A), and those that feature a steep or near-vertical cliff in the vicinity of the shoreline (type-B).

While the southeast Australian coastline (Figure 1) is best known for its extensive and diverse sandy beach systems (Short, 2006), rocky shores make up about 36% of the open-coast New South Wales (NSW) coastline. Rocky shores are more prevalent in central and southern NSW relative to northern NSW. In the central and south, the steep continental margin and rugged coastal geology of the Sydney Basin and Lachlan Fold Belt have restricted the development of sandy beaches to relatively narrow coastal embayments, whereas in the north, subdued coastal geology has supported the development of extensive sandy beaches that are intermittently divided by short stretches of rocky shore bordering headlands (Roy and Thom, 1981).

There is growing awareness in Australia that historically there has been a perhaps disproportionate focus on identifying and managing recreational swimming hazards and associated risks on sandy beaches, whereas recreational activities on rocky shores contribute a disproportionately high number of injuries and deaths relative to the numbers of recreational users (Kennedy et al., 2013).

In this paper we investigate wave processes and overwash hazards at Figure Eight rock platform in southeastern Australia. The platform features unique geomorphology that contributes to its natural beauty and hazardous nature. A rapid increase in visitation driven by social media use, and a coincident increase in visitor injuries, has prompted efforts to improve the management of visitor safety. In contrast to traditional ideas of rocky shore hazards, where injuries and deaths arise from victims being washed into the sea, injuries at Figure Eight chiefly arise from visitors being dragged landward across the platform by overwash waves.

¹Water, Wetlands and Coasts Science, Office of Environment and Heritage, NSW Government, 59 Goulburn Street, Sydney 2000, New South Wales, Australia. Michael.Kinsela@environment.nsw.gov.au

²School of Environmental and Life Sciences, Faculty of Science and IT, The University of Newcastle, University Drive, Callaghan 2308, New South Wales, Australia. Hannah.Power@newcastle.edu.au

2. Figure Eight Rock Platform

The Figure Eight rock platform is a high visitation and hazardous natural attraction located in the Royal National Park, about 1 hour south of Sydney, Australia (Figure 1). The site features a variety of unique natural rock pools, including the namesake Figure Eight Rock Pool, which have been weathered into the sandstone platform over thousands of years. Despite challenging access via a steep escarpment trail and rocky shore traverse (minimum 2 hours return walk), the rock pools attract a high volume of local and international visitors, who primarily visit to bathe in the pools and have their photo taken. The hazardous setting, unique morphology and high visitation present challenges to managing visitor safety at the site.

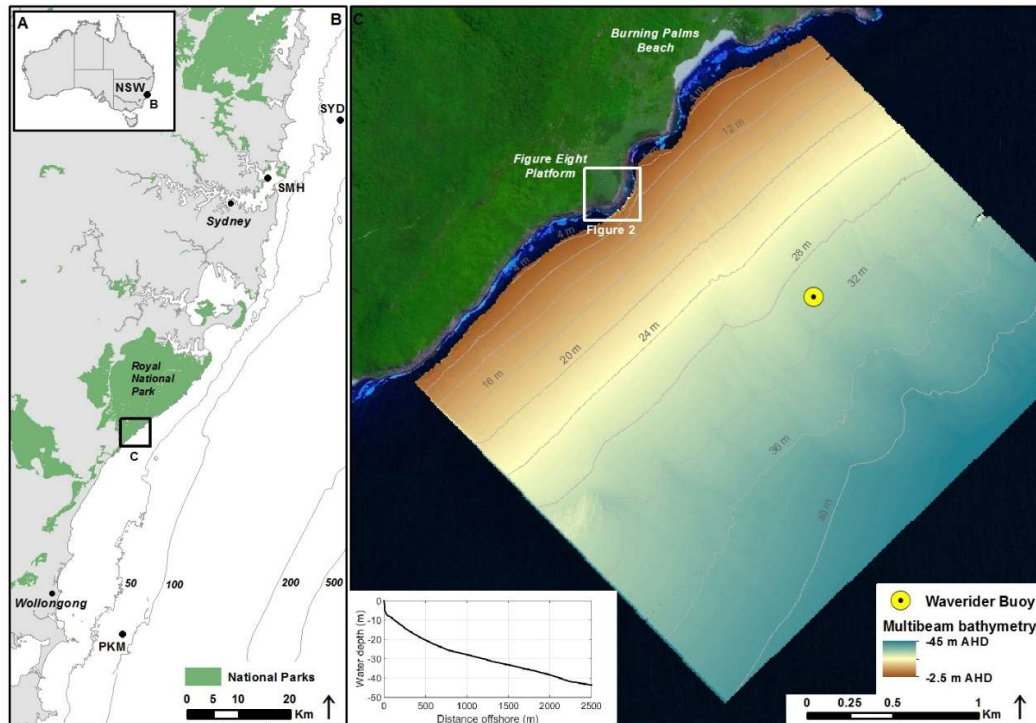


Figure 1. The Figure Eight rock platform is located in the Royal National Park about 50 km south of Sydney, Australia. The coastline trends northeast-southwest and is fully exposed to waves arriving from the northeast to south directions.

Directional waverider buoys are maintained at Sydney (SYD) and Port Kembla (PKM), and an ocean tide gauge at Middle Head in Port Jackson (SMH). A directional waverider buoy was deployed in 30 m water depth adjacent to the Figure Eight rock platform to measure local wave conditions. The bathymetry profile runs SE out from the platform.

2.1. Geomorphology and processes

The Figure Eight rock platform is a relatively flat and wide intertidal to supratidal sandstone platform with a curved northeast-southwest orientation that fringes coastal cliffs of 40 m elevation (Figure 2). The platform extends 50 m on average from the base of the cliffs to the shore, where it drops abruptly into the sea. The seaward edge of the platform is near-vertical and well defined in the vicinity of the mean sea-level shoreline, reflecting the 'type-B' platform (Sunamura, 1992; Kennedy, 2015). The water depth at the seaward edge is around 5 m, and the nearshore seabed slopes steeply to around 7-8 m. The inner-continental shelf fronting the platform has an average slope of 1:50 out to 50 m water depth (Figure 1C), and an inner-shelf sand body has been reported along this coastal sector (Field and Roy, 1984). The escarpment, cliffs and rock platform form part of the East Australian marine abrasion surface, formed of Mesozoic-Palaeozoic sedimentary rocks cut and planed by cyclic marine erosion, which extends 300 km along the coast north and south of Sydney and up to 23 km offshore (180 m below sea level) beneath continental shelf sediments (Thom et al., 2010).

The topography of the platform is complex, with the northeast section higher than the southwest section, and the seaward edge often higher than the mid-platform elevation (Figure 2). While platform elevation is generally above the highest astronomical tide – around 1 m above Australian Height Datum (AHD), which approximates mean sea level – in this microtidal setting (2 m maximum tidal range), the platform is exposed to the full range of wave directions (northeast to south) within a moderate-high energy wave climate (mean $H_{sig}=1.6$ m, $T_{sig}=8$ s). The irregular elevation and form of the seaward edge exposes the platform to overwash and inundation caused by waves predominantly arriving from south to southeast directions.

The complex platform morphology, elevation relative to the tidal range, and moderate-high energy wave climate, collectively suggest that hydrodynamic conditions across most of the platform can vary between three primary states: (1) no overwashing; (2) partial-intermittent overwashing; and, (3) complete inundation.

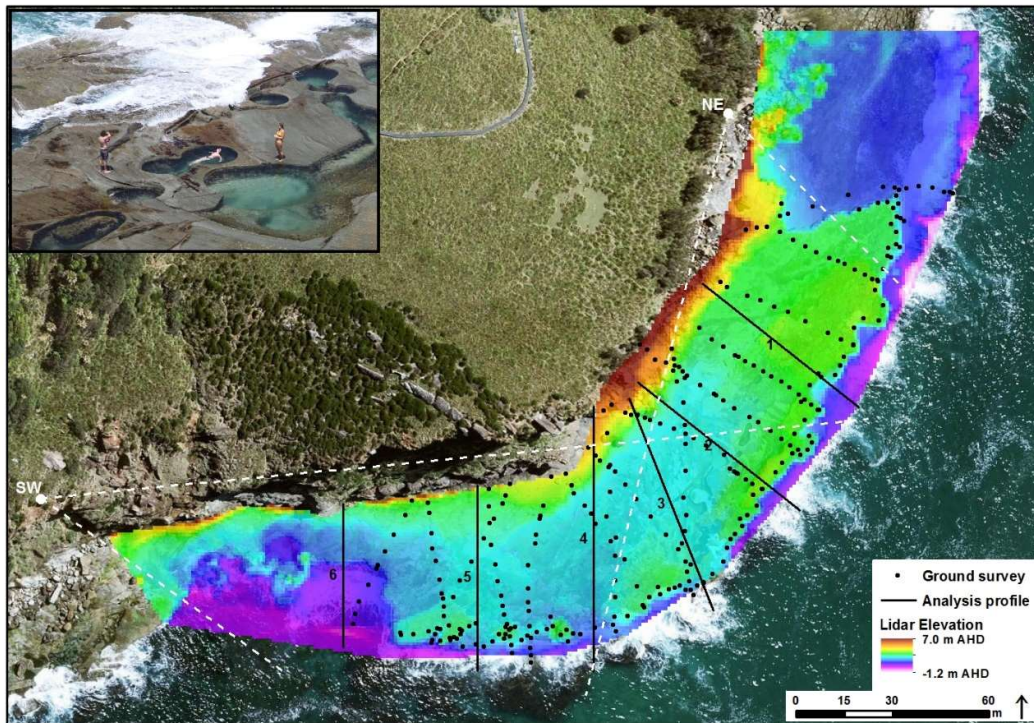


Figure 2. Morphology of the Figure Eight rock platform as captured by airborne Lidar data. See Figure 1C for location. The northeast (NE) and southwest (SW) camera positions and fields of view are indicated in white, and the camera image analysis profiles and ground topography survey points are also shown. Inset shows typical visitor behaviour.

2.2. Visitation and hazards

Although the rock platform and pools have always been accessible to the public, visitation has been relatively low in the past due to limited public awareness, and challenging access to the remote location via a steep escarpment trail and rock-platform traverse. Visitation has increased rapidly in the past 2 years following popularisation of the site on social media networks. For example, data from the primary access trail suggests that monthly average visitation during spring-summer months has increased from around 2,500 in 2014/15, to over 5,000 visits per month in 2015/16, and 7,500 visits per month in 2016/17.

The primary activity of visitors to the Figure Eight rock platform is to bathe in the natural rock pools and have their photo taken. The proximity of the pools to the seaward edge of the platform means that visitors are often exposed to overwash, generated when ocean waves collide with or break onto the platform, often resulting in lacerations and impact injuries. In more severe incidents, visitors suffering broken bones or head injuries have required evacuation by rescue helicopter. The intrinsically dangerous location, time-varying

overwash wave hazards, and visitor behavior, present complex challenges to managing visitor safety.

3. Methods

3.1. Terrain surveys

The topography of the rock platform was captured in an airborne Lidar survey carried out by New South Wales Land and Property Information (LPI) in 2013, which is presented as a 1 m grid in Figure 2 (horizontal accuracy 0.8 m, vertical accuracy 0.3 m – 95% CI). Considering the complex morphology of the site, a ground topography survey was carried out using a Leica real-time kinematic GNSS system to ground-truth the 1 m gridded Lidar data. The sampling pattern for the ground survey is shown in Figure 2.

Existing hydrographic and seabed data covering the inner-continental shelf along this section of coast was relatively poor due to the distance from major ports and the sparsely inhabited location within a national park. A bathymetry and backscatter survey of the inner-continental shelf adjacent to the platform was carried out using an R2Sonic 2022 multibeam echosounder system, to build a detailed model of the seabed out to 45 m water depth (Figure 1). The dataset provides new detail on the geomorphology of the shoreface and near-platform seabed and will support high-resolution nearshore wave modelling (not presented here). Sediment grab samples were also retrieved in 10, 20, 30, 40 and 50 m water depth to support backscatter data analysis.

3.2. Wave climate analysis

Permanent deep-water waverider buoy deployments are maintained in about 80 m water depth off the coasts of Sydney and Port Kembla (Figure 1B). The Sydney wave buoy has collected directional wave data since 1992, while the Port Kembla buoy was upgraded to a directional instrument in 2013 (non-directional wave measurement extends back to the mid-1970s in both areas). The most reliable ocean tide gauge in the region is the Sydney Middle Head tide gauge located directly inside the entrance to Port Jackson (Figure 1B).

A Datawell DWR-G4 waverider buoy was deployed in 30 m water depth adjacent to the Figure Eight rock platform (Figure 1C) to measure local wave conditions throughout the period of camera monitoring and hydrodynamic measurements. The buoy was first deployed on 6 December 2016 and is serviced every 5 weeks to de-foul the hull, replace the batteries and retrieve the data. The deployment is ongoing.

Directional wave data was also derived at the 30 m wave buoy location using the [NSW Nearshore Wave Transformation Tool](#) (NWTT), which uses advanced parametric and spectral wave transformation functions that rapidly transfer offshore wave conditions to virtual buoys along the entire NSW coastline (Taylor et al., 2016; Baird Australia, 2017). The offshore wave data is from the NSW deep-water waverider buoy network, and a global-regional ocean wave hindcast dataset that has been developed using the WAVEWATCH® III model and Climate Forecast System ocean-atmosphere forcing (Kinsela et al., 2014).

The wave data were analysed to investigate the nature of wave conditions at the Figure Eight rock platform relative to the regional offshore wave climate. The performance of the wave transformation tool at the Figure Eight 30 m wave buoy location was evaluated against measured wave data at that location.

3.3. Hydrodynamic observations

A coastal camera monitoring system was installed at the site to collect a dataset of platform hydrodynamic conditions for the range of tide and wave conditions experienced during the sampling period. The cameras were installed in March 2017 and monitoring will continue for a minimum period of 3 months. Considering platform curvature and the high coastal cliffs, cameras were installed in two locations in elevated positions to capture the primary area of interest for observing wave overwash processes (Figure 2).

The camera systems comprised 3.2 megapixel Point Grey Flea3 colour image cameras fitted with Fujinon 6 mm lenses. Solar-battery power supply systems were installed at both sites to provide sufficient power under the range of potential weather conditions. The cameras are operated automatically by Raspberry Pi computers that store the image data on USB flash drives. Mobile telephone network modems were also fitted to telemeter sample images and system information at each capture cycle for monitoring. The computers were configured to capture images at 1 Hz for 20 minutes from the beginning of each daylight hour.



Figure 3. Photos of the southwest (left) and northeast (right) camera system installations. See Figure 2 for locations.

Timex and variance images were generated from the raw image series collected by each camera during each 20-minute capture cycle. Raw images were rectified using ground control points that were measured using a Trimble real-time kinematic GNSS system, to detect overwash wave processes at x/y coordinate positions for each pixel, and enable profile-based timestack analysis.

Timestack analysis was carried out for each pixel along each image analysis profile (Figure 2) to identify the presence and extent of wave overwashing along each profile in each image. Pixel values were interrogated against thresholds that were calibrated to distinguish overwash waves from natural surfaces (e.g. exposed rock platform, ponded water in pools or on the platform surface, algae) for the range of light conditions experienced during sampling. %-time-overwashing (pixel lightness) plots were derived to calculate and visualise the proportion of each 20-minute capture cycle that each individual pixel position along each profile was subject to wave overwash. The pixel overwash time plots therefore describe the combined extent and duration of wave overwashing along each profile for each capture cycle.

Hydrodynamic sampling was carried out across the platform during a range of conditions to verify the camera data and investigate the intensity and forces associated with overwash waves under different tide and wave conditions. Pressure sensors were deployed in rock pools along several transects across the platform over tidal cycles and through a range of storm and swell events (data not reported here).

3.4. Preliminary overwash hazard analysis

A first-pass overwash hazard model was developed to support visitor safety management prior to completion of the camera monitoring data collection and analysis (Section 3.3). The first-pass model predicts platform overwashing using ocean tide and transformed wave height (30 m wave buoy location) information only, and will be evaluated against the complete camera monitoring dataset (a subset of the dataset is considered here).

The first-pass model applies the EurOtop relative wave run-up ($R_{u2\%}$) relationship for coastal dikes and embankment seawalls (EurOtop, 2016; Victor et al., 2012), assuming that the seaward edge of the Figure Eight platform can be approximated by a vertical wall, and therefore adopting a relative wave run-up level ($R_{u2\%}/H_{m0}$) value of 1.8. The relationship was applied using the combined ocean tide and wave height water level to account for the influence of the tide level on platform overwashing.

4. Results

4.1. Platform geomorphology

Comparison between the 1 m gridded Lidar data captured in 2013 and the ground survey carried out using a Leica real-time kinematic GNSS system (Figure 2), gave a root-mean-square deviation of 0.18 m based on

the nearest neighbor sampling method. Manual comparison between individual survey points and Lidar grid pixels overlaid on aerial imagery indicated that deviation between the two primarily resulted from averaging of complex topography within the 1 m resolution grid pixels.

Figure 4 shows Lidar-derived terrain profiles for the six cross-shore image analysis profiles (Figure 2), and alongshore terrain profiles taken along the middle and seaward edge of the platform. The topography of the seaward edge varies along the platform. The southwest (SW) half of the platform features a lower seaward edge of highly variable elevation between 1-2 m AHD. The northeast (NE) half of the platform features a more consistent higher seaward edge between 2-3 m AHD elevation. Landward of the seaward edge platform elevation is typically at or below the seaward edge. Of particular interest, Profile 2, which intersects the namesake Figure Eight rock pool, features a seaward edge around 1 m higher than the mid-platform elevation.

With the exception of the sector in the vicinity of Profile 6, platform elevation is typically above the still-water mean spring high tide and highest astronomical tide levels (Figure 4). This is reflected in Figure 2 as platform surfaces that are shaded light blue, green, or warmer colours.

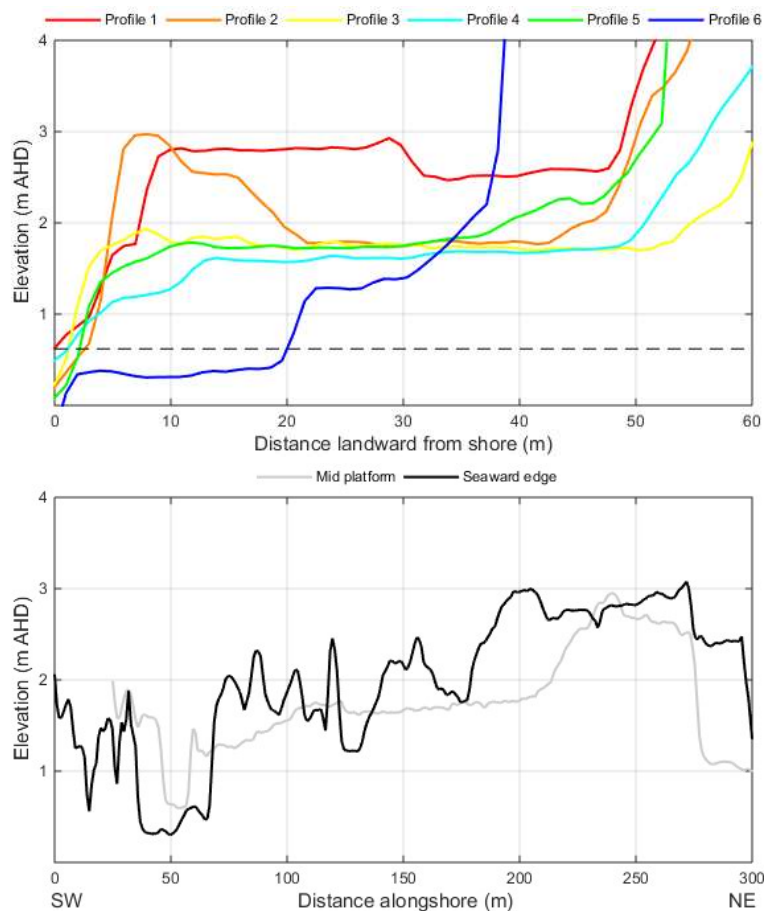


Figure 4. Lidar-derived terrain profiles for the six image analysis profiles shown in Figure 2 (top), and alongshore terrain profiles taken along the middle and seaward edge of the platform (bottom). Dashed line is mean high water.

The inner-continental shelf seabed fronting the platform was confirmed to be primarily composed of quartz sand consistent with that of the shelf sand body further to the north described by Field and Roy (1984). The shoreface was found to have regular concave geometry with an average slope of 1:65 between the vicinity of the platform seaward edge (7 m water depth) and 40 m water depth (Figure 1). Shore-transverse bedforms of 0.5-1 m relief occur across the relatively uniform mid shoreface, between 10-25 m water depths, while the lower shoreface features irregular morphology perhaps related to drainage features and currents (Figure 1).

4.2. Wave climate analysis

Figure 5 shows offshore and nearshore wave data from the study area for the period December 2016 to March 2017, including the first 3 months of the wave buoy deployment adjacent to the Figure Eight rock platform (Figure 1). Visual comparison between the offshore observations at the Port Kembla 80 m buoy (black), and at the Figure Eight 30 m buoy (green), suggest that nearshore wave heights are slightly lower than offshore, while wave period and direction appear comparable between the stations.

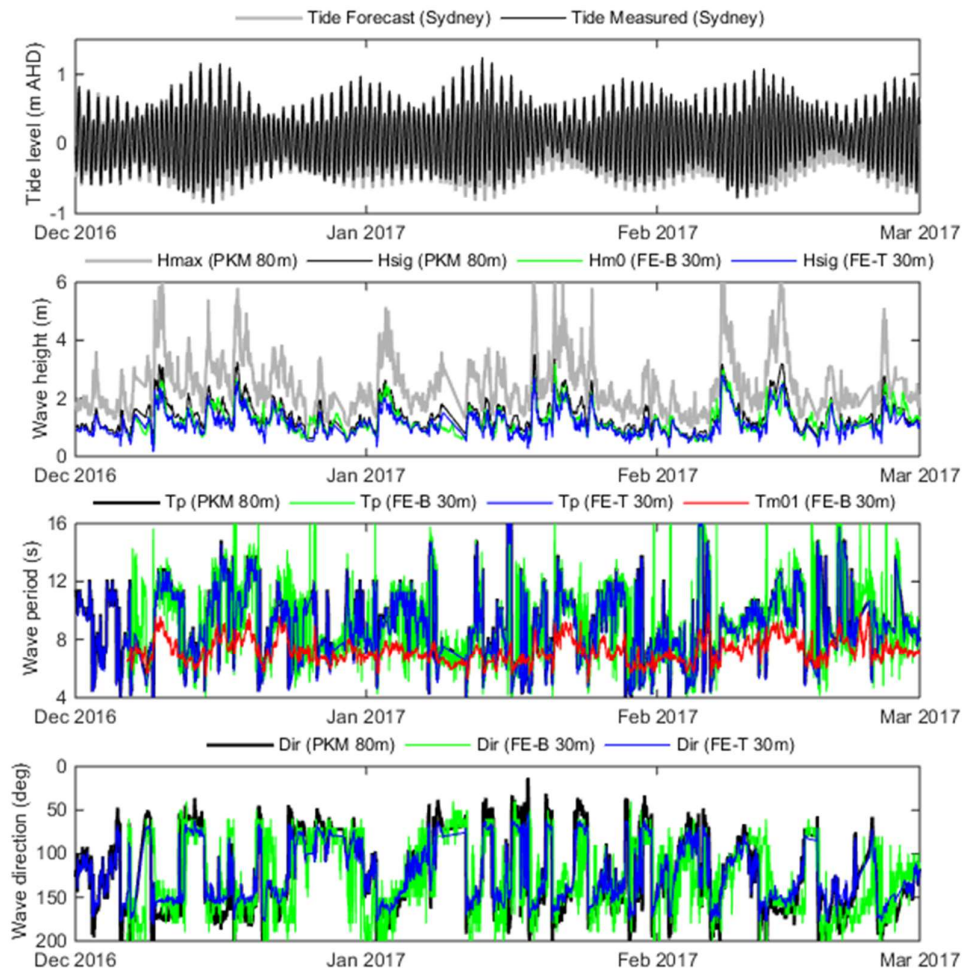


Figure 5. Ocean tide (Sydney), offshore waves (Port Kembla: PKM), measured nearshore waves (Figure Eight: FE-B) and transformed nearshore waves (Figure Eight: FE-T) for 12/2016 to 3/2017. See Figure 1 for station locations.

At the Figure Eight wave buoy, measured significant wave height (H_{m0}) exceeded 2 m for 17% of the total buoy deployment period to date (6/12/2016-27/3/2017), and exceeded 3 m for 2.5% of the time. Figure 6 (left) compares significant wave height measured at the Port Kembla 80 m buoy and at the Figure Eight 30 m buoy for the period shown in Figure 5. The comparison shows that wave height attenuation from the mid to inner shelf increases with increasing wave height. The Port Kembla wave buoy was out of service during March 2017 and so Figure 5 and Figure 6 only show wave data for the period 6/12/2016-1/3/2017.

Figure 5 also suggests that transformed wave predictions from the NWTT (blue) provide a good predictor of measured wave conditions at the Figure Eight 30 m buoy location (green). Figure 6 (right) compares the transformed wave height from the NWTT with measured wave height at the Figure Eight 30 m buoy, for the 3-month period shown in Figure 5. The root-mean-square error and bias are 0.26 and -0.085 respectively.

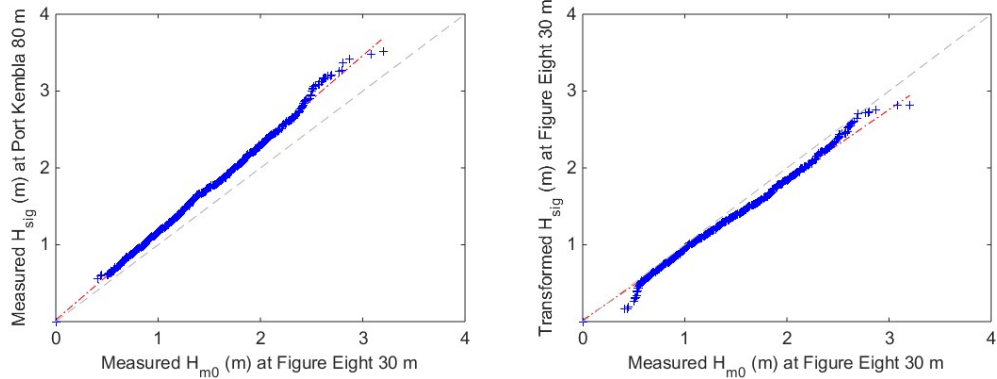


Figure 6. Quantile-quantile plots comparing significant wave height measured at the Port Kembla 80 m wave buoy and Figure Eight 30 m wave buoy (left), and comparing transformed (NWTT) and measured significant wave height at the Figure Eight 30 m wave buoy location (right), for the 3-month period shown in Figure 5.

Inspection of the tide and wave data shown in Figure 5 suggests that a wide range of conditions have been sampled at the Figure Eight 30 m buoy location. Figure 7 shows wave height-direction polar plots based on 4 years of directional observations at the Port Kembla 80 m buoy, and 4 months of observations at the Figure Eight 30 m buoy. The comparison indicates a relatively consistent sampling of ENE, ESE and SE wave directions at the Figure Eight 30 m buoy during that period, with the highest wave conditions arriving from the predominant ESE and SE directions. The comparison also confirms that the Figure Eight rock platform is exposed to the full range of wave directions experienced in this region.

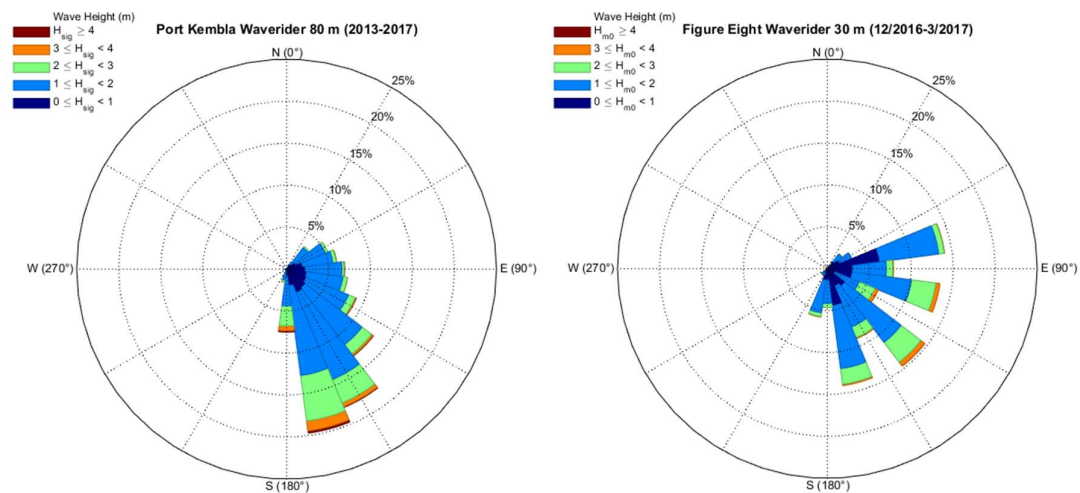


Figure 7. Wave height-direction polar plots for data from the Port Kembla 80 m wave buoy (2013-2017) and the Figure Eight 30 m wave buoy (6/12/2016-27/3/2017) deployments. See Figure 1 for station locations. Credit: WindRose.m.

4.3. Hydrodynamic observations

As anticipated from the consideration of platform morphology and regional wave and tide data, preliminary analysis of the camera image data confirms that the Figure Eight rock platform is subject to the full spectrum of potential hydrodynamic conditions, which are categorised here as: (1) no overwashing; (2) partial-intermittent overwashing; and, (3) complete inundation. Figure 8 shows examples of each of the three hydrodynamic conditions as captured by the camera monitoring systems. The three conditions can be differentiated on the basis of the frequency, duration and extent of wave overwashing across the platform.

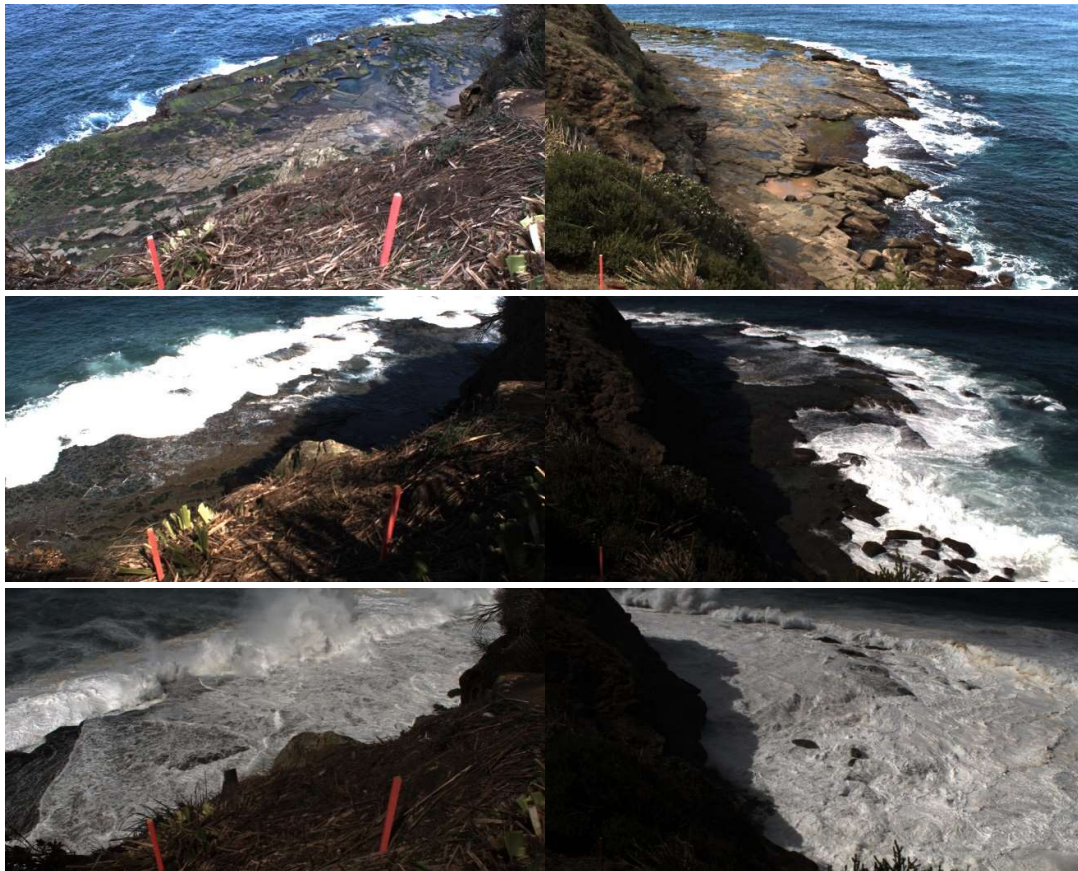


Figure 8. Camera monitoring images showing: no overwashing (top), partial-intermittent overwashing (middle) and complete inundation (bottom) conditions at Figure Eight rock platform. Images from the northeast (left) and southwest (right) cameras (Figure 2) were captured simultaneously and together show the platform in view under each condition.

Figure 9 shows example %-time-overwashing (pixel lightness) plots for partial-intermittent overwashing conditions characterised as nuisance (left) and hazardous (right) overwashing. The plots show the proportion of time and extent of overwashing at profile 2 (Figure 2) during a 20-minute capture cycle. Threshold %-time-overwashing profiles will be derived from the full dataset to identify platform hydrodynamic conditions.

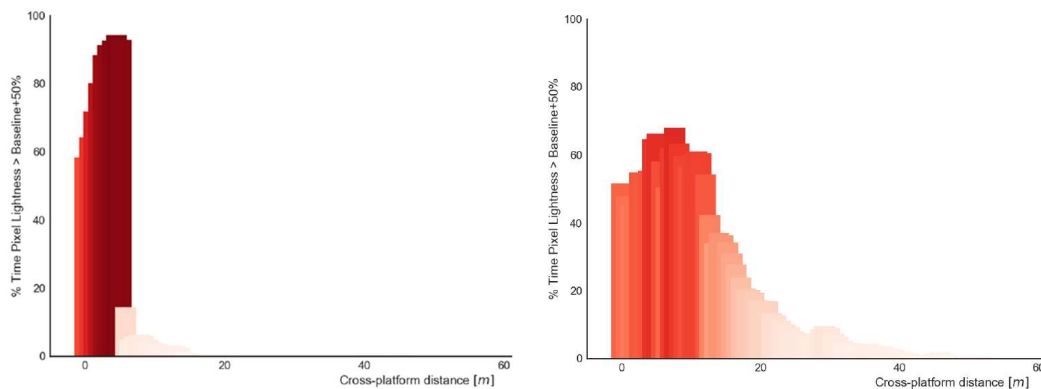


Figure 9. Example %-time-overwashing plots for partial-intermittent overwashing conditions featuring nuisance (left) and hazardous (right) overwashing. For the conditions on the left overwash is restricted to the vicinity of the seaward edge, while overwash waves frequently extend across the platform during the conditions on the right.

4.4. Preliminary overwash hazard analysis

Figure 10 shows combined ocean tide and wave water levels for the first 4 months of the Figure Eight wave buoy deployment (6/12/2016-27/3/2017). The difference between the ocean tide and wave height level (black) and ocean tide and relative wave run-up level (grey) represents the influence of overwash processes predicted by the first-pass hazard model. The 2 m (orange) and 3 m AHD (red) platform elevation thresholds represent indicative platform overwash levels for profiles 3-5 and profiles 1-2 respectively (Figure 4).

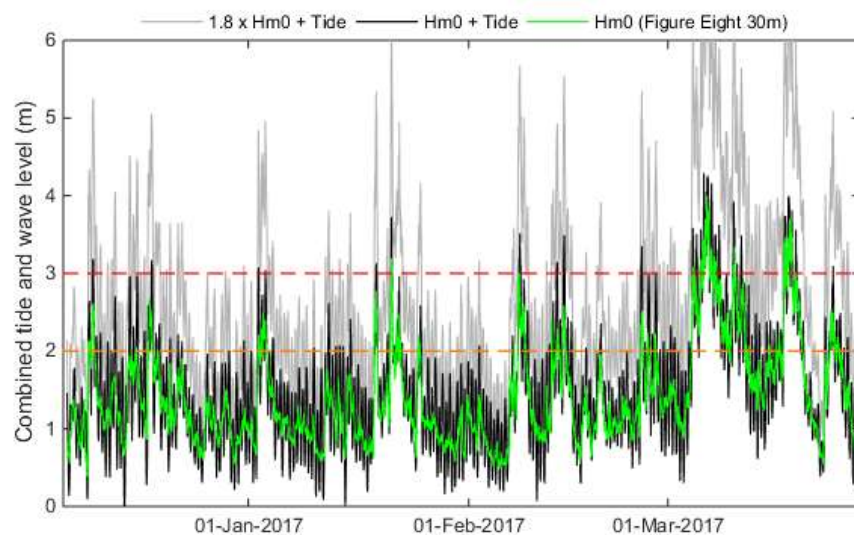


Figure 10. Significant wave height (H_{m0}) measured at the Figure Eight 30 m wave buoy (green), combined ocean tide and wave height water level (black), and combined ocean tide and relative wave run-up level ($R_{u2\%} = 1.8 \times H_{m0}$; grey). The orange and red lines indicate 2 m and 3 m AHD platform elevation thresholds (see Figure 4).

The data shown in Figure 10 indicates that the combined ocean tide and wave height water level (black) was typically below the 2 m AHD platform elevation threshold, and only exceeded the 3 m AHD elevation threshold on several occasions during the 4-month period. Table 1 shows %-time-elevation exceedance values for the water and run-up levels shown in Figure 10 (Measured H_{m0}). While the combined ocean tide and wave height water level ($H_{m0} + \text{Tide}$) only exceeded the 2 m and 3 m AHD elevation thresholds 22% and 4.8% of the observation period, the ocean tide and relative wave run-up level ($1.8 \times H_{m0} + \text{Tide}$) exceeded the same elevation thresholds 66% and 30% of the time respectively.

Table 1. %-time-elevation exceedance values for the combined ocean tide and wave height water level and ocean tide and relative wave run-up level ($R_{u2\%}$) data shown in Figure 10 (6/12/2016-27/3/2017).

Platform elevation threshold	%time-elevation threshold exceedance	
	$H_{m0} + \text{Tide}$	$1.8 \times H_{m0} + \text{Tide}$ ($R_{u2\%}$)
≥ 3 m AHD	4.8%	30%
≥ 2 m AHD	22%	66%
≥ 1 m AHD	73%	97%

5. Discussion

The unique and complex morphology of the Figure Eight rock platform appears to be a contributing factor to the hazardous nature of the site. First, average platform elevation relative to the local tide range and wave climate allows hydrodynamic conditions across the platform to vary between three primary states for a range

of ordinary wave conditions (Figure 8): (1) no overwashing; (2) partial-intermittent overwashing; and, (3) complete inundation. Second, both alongshore and cross-shore variability in platform morphology (Figures 2 & 4) suggest that the nature of partial-intermittent overwashing conditions may vary depending on the combined ocean tide and wave water level, and wave direction. Third, the highly variable morphology of the seaward edge (Figure 4) means that the frequency and intensity of overwashing may be unpredictable during partial-intermittent conditions, depending on how individual incident waves interact with the seaward edge. Lastly, the elevated seaward edge along the most visited part of the platform (Profile 2, Figure 4) means that visitor's views of the ocean and incident waves is restricted when bathing in the pools in that area.

In terms of managing visitor safety, partial-intermittent overwashing conditions present the greatest challenge. This is due to the complex and unpredictable nature of those conditions, as described above, and an apparent reduction in the perceived risk of wave overwash hazards. For example, comparison between emergency response data from 2016 and measured offshore wave conditions, indicates that the majority of major incidents occurred when offshore significant wave height was around 2 m (i.e. near modal conditions for this coast), which is associated with partial-intermittent overwashing (Figure 10). During these conditions, wave height is low enough for the danger of overwash to be less apparent than during frequent or complete inundation. The first-pass overwash hazard model based on the combined ocean tide and relative wave run-up level exceeded 2 m AHD – i.e. the average elevation of much of the platform (Figure 4) – for 66% of the initial 4 months of the Figure Eight 30 m wave buoy deployment, and exceeded 3 m AHD for only 30% of that same period (Table 1). During inundation conditions, when the wave run-up level constantly exceeds 3 m AHD, the platform is inaccessible due to continuous and complete overwashing (Figure 8).

The first-pass overwash hazard model, based on the combined ocean tide and relative wave run-up ($R_{u2\%}$) level, provides some initial insights on overwash wave processes and hazards at the Figure Eight rock platform. For example, the %-time-elevation exceedance values (Table 1) for combined ocean tide and wave height water level (black, Figure 10) suggest that without wave overwash and run-up processes, the platform would rarely experience overwashing or inundation. However that is contrary to preliminary analysis of the camera data. Figure 11 shows the final week of combined ocean tide and wave water levels presented in Figure 10, which coincided with the initial week of camera monitoring. The vertical colour bars indicate the hydrodynamic conditions observed by the cameras at Profile 2 in daylight hours. Conditions are categorized as no overwashing (grey), and 3 levels of partial-intermittent overwashing: nuisance (yellow), hazardous (orange), and extreme (red). At the Figure Eight rock pool, situated about 15 m from the seaward edge of the platform on Profile 2 (Figure 2), nuisance overwashing featured small overwash waves that only just reached the pool, hazardous overwashing featured moderate overwash waves washing through the pool, and extreme overwashing featured large overwash waves regularly washing completely across the visible platform.

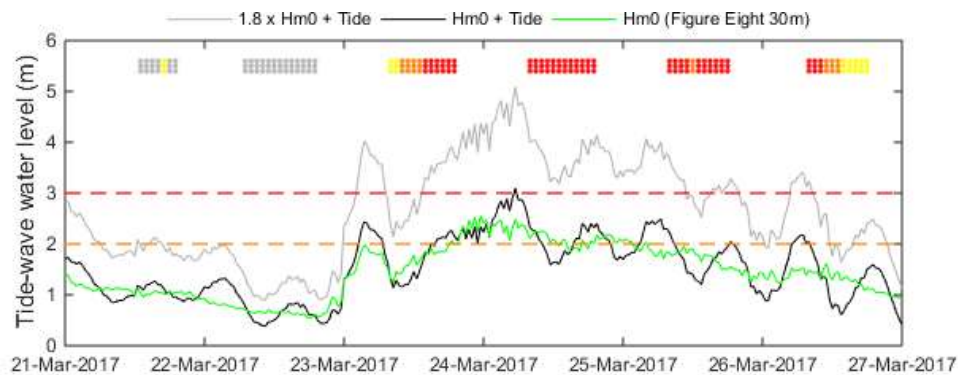


Figure 11. Combined ocean tide and wave water levels (see Figure 10 caption) covering the initial week of camera monitoring. Vertical colour bars at top indicate hydrodynamic conditions observed by the camera systems (see text).

The comparison in Figure 11 suggests that the first-pass overwash hazard model based on the ocean tide and relative wave run-up level (grey) provides a reasonable indicator of overwashing. For example, when below the 2 m AHD threshold platform overwashing was absent (grey) or nuisance (yellow), when between 2-3 m AHD overwashing was hazardous (orange), and when above 3 m AHD overwashing was extreme (red).

The wave climate analysis confirmed that the Figure Eight rock platform is exposed to the full spectrum of wave directions (northeast to south) experienced in this region (Figure 7), and that wave height attenuation from the mid to inner shelf increases with increasing wave height (Figure 6). Furthermore, the transformed significant wave height predicted by the NSW Nearshore Wave Transformation Tool at the Figure Eight 30 m buoy location compared well with measured wave heights (Figure 6). This suggests that once the combined ocean tide and relative wave run-up thresholds for overwashing have been refined and verified at Figure Eight rock platform using the camera monitoring data, measured and projected ocean tide data and the wave transformation tool may be used to provide real-time and forecast overwash hazard advice, based on real-time offshore wave buoy data and a deep-water ocean wave forecast.

The detection of overwash waves and classification of platform hydrodynamic conditions using the camera system and image analysis techniques described here will be continued for several months to develop a dataset covering a diverse range of wave conditions as measured at the Figure Eight 30 m wave buoy. The dataset will be analysed to expand and refine the thresholds used to differentiate the platform hydrodynamic conditions. To further understand variation in the frequency and intensity of partial-intermittent overwashing conditions in particular, the imagery dataset will be compared with hydrodynamic data collected by pressure sensors that are being deployed across the platform during a range of tide and wave conditions. Nearshore wave sensor deployments and high-resolution wave modelling are also being carried out to develop and improved understanding of wave transformation from the 30 m wave buoy to the platform edge.

Acknowledgements

The authors thank the NSW National Parks and Wildlife Service for assisting with the design, installation and maintenance of the camera and power systems, and support provided to carry out the data analysis and research presented here. We also thank the Sydney Institute of Marine Science (SIMS) and Water Research Laboratory (UNSW Sydney) for the collaborative use of Datawell DWR-G4 wave buoy instruments. Manly Hydraulics Laboratory provided ocean tide and deep-water wave data for Sydney and Port Kembla.

References

- Baird Australia, 2017. NSW Coastal Wave Model – Statewide Nearshore Wave Transformation Tool. Prepared by Baird Australia for the Office of Environment and Heritage, NSW Government.
- EurOtop, 2016. Manual on wave overtopping of sea defences and related structures. An overtopping manual largely based on European research, but for worldwide application. Van der Meer, J.W., Allsop, N.W.H., Bruce, T., De Rouck, J., Kortenhaus, A., Pullen, T., Schüttrumpf, H., Troch, P. and Zanuttigh, B., www.overtopping-manual.com.
- Field, M.E. and Roy, P.S., 1984. Offshore transport and sand-body formation: Evidence from a steep, high-energy shoreface, southeastern Australia. *Journal of Sedimentary Petrology*, 54(4): 1292-1302.
- Kinsela, M., Taylor, D., Treloar, D., Dent, J., Garber, S., Mortlock, T., Goodwin, I., 2014. NSW Coastal Ocean Wave Model: Investigating Spatial and Temporal Variability in Coastal Wave Climates. *Proceedings of the 23rd NSW Coastal Conference*, 11-14 November, Ulladulla.
- Kennedy, D.M., Sherker, S., Brighton, B., Weir, A. and Woodroffe, C.D., 2013. Rocky coast hazards and public safety: moving beyond the beach in coastal risk management. *Ocean & Coastal Management*, 82:85-94.
- Kennedy, D.M., 2015. Where is the seaward edge? A review and definition of shore platform morphology. *Earth-Science Reviews*, 147:99-108.
- Roy, P.S. and Thom, B.G., 1981. Late Quaternary marine deposition in New South Wales and southern Queensland - An evolutionary model. *Journal of the Geological Society of Australia*, 28: 471-489.
- Short, A.D., 2006. Australian beach systems – nature and distribution. *Journal of Coastal Research*, 22: 11-17.
- Sunamura, T., 1992. *Geomorphology of Rocky Coasts*, Wiley, Chichester.
- Taylor, D., Garber, S., Burston, J., Couriel, E., Modra, B. and Kinsela, M., 2015. Verification of a Coastal Wave Transfer Function for the New South Wales Coastline. *Proceedings of Australasian Coasts and Ports Conference*, 15-18 September 2015, Auckland.
- Thom, B.G., Keene, J.B., Cowell, P.J. and Daley, M., 2010. East Australian marine abrasion surface, in Bishop, P. and Pillans, B. (eds) *Australian Landscapes*, Geological Society, London, Special Publications, 346: 57-69.
- Victor, L., van der Meer, J.W. and Troch, P., 2012. Probability distribution of individual wave overtopping volumes for smooth impermeable steep slopes with low crest freeboards, *Coastal Engineering*, 64: 87-101.